

Titanium Diboride–Derived Nanosheet Coatings for Enhanced Condensation Heat Transfer

Bhagyashri Gaykwad^a, Sakshi Katkur^a, Arunima Roy^b, Soumyadip Sett^{*b}, and Kabeer Jasuja^{*a}

^a *Department of Chemical Engineering, Indian Institute of Technology Gandhinagar, Palaj, Gandhinagar, Gujarat 382055, India*

^b *Department of Mechanical Engineering, Indian Institute of Technology Gandhinagar, Palaj, Gandhinagar, Gujarat 382055, India*

Electronic Supplementary Information (ESI)

1. Detailed steps of synthesis of TiB₂-derived nanosheets (TNS)

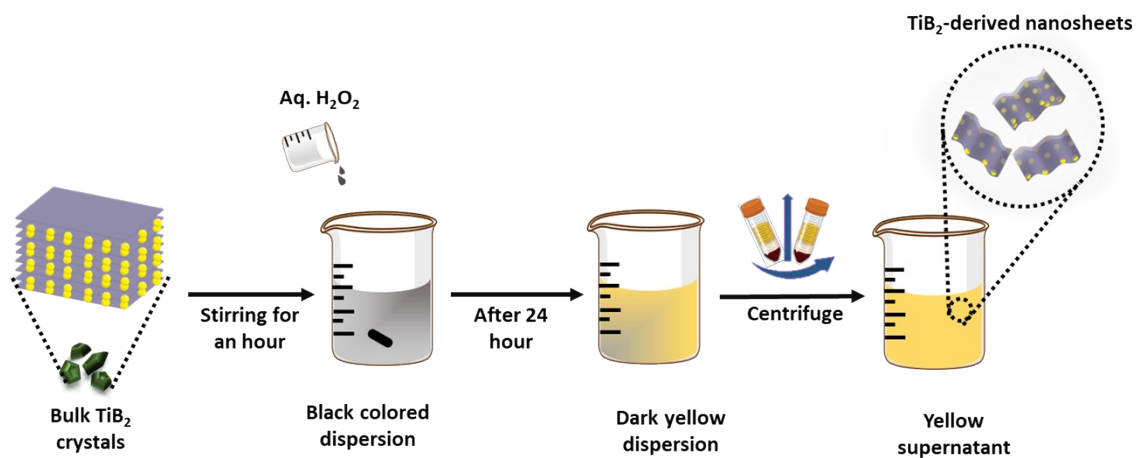


Figure S1: Dissolution and recrystallization recipe to synthesize TiB₂-derived nanosheets as reported by James et al.¹

2. APTES molecule structure

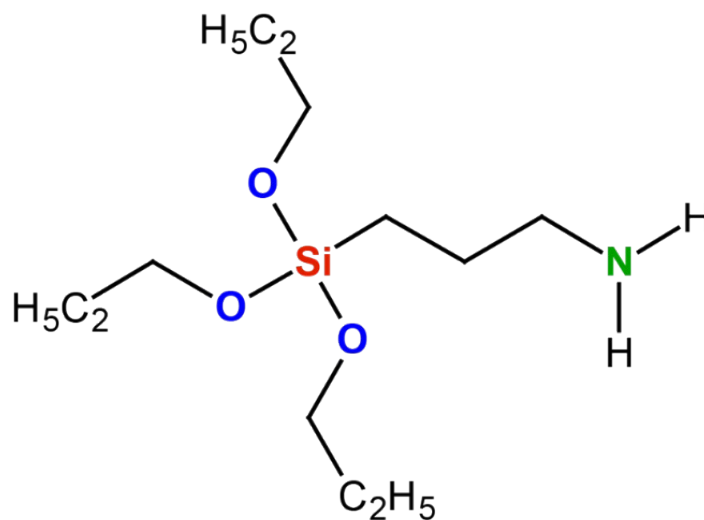


Figure S2: APTES molecule structure

3. Experimental Setup for Condensation Experiments

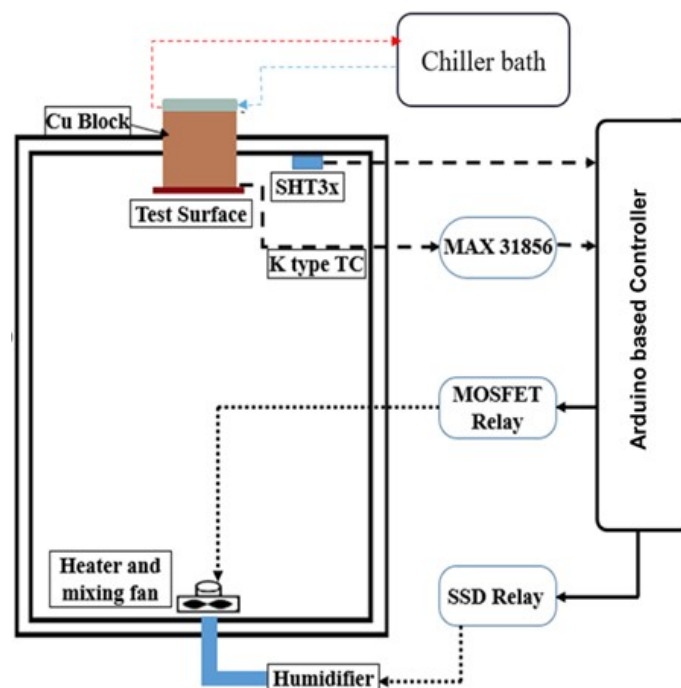


Figure S3: Schematic of the experimental setup for vapor condensation experiments in a controlled environment.

4. XPS Analysis of bare Cu, silanized Cu, and TNS-coated Cu

- XPS survey scan of bare Cu, silanized Cu, and TNS-coated Cu

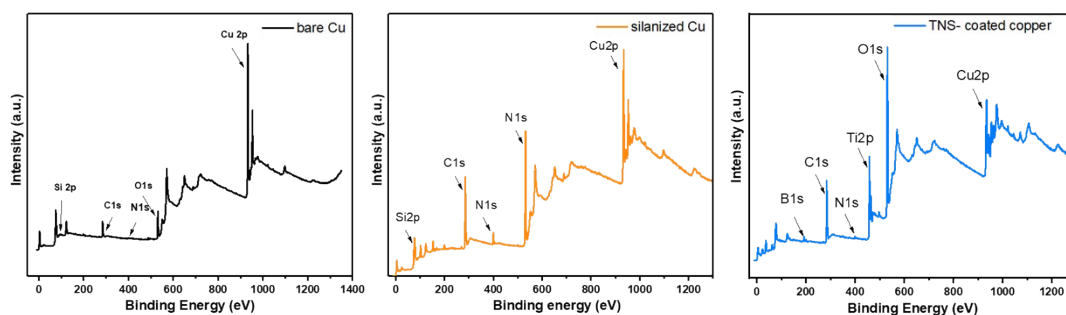


Figure S4: XPS survey spectra of bare Cu, silanized Cu, and TNS-coated Cu.

- XPS spectra of bare Cu

The XPS spectra of bare Cu is shown in Figure S5, the Cu 2p_{3/2} signal is deconvoluted into three peaks: the first peak at 932.8 eV corresponds to the metallic Cu, and the second and third peaks at 947.1 and 952.8 eV are attributed to CuO species. The O1s spectra at 530.8 eV also confirm the existence of CuO species. The other peak at 532.1 eV in the same XPS spectra is attributed to the presence of a hydroxyl group on the Cu surface. This -OH group

signifies the successful hydroxylation of Cu after acid treatment. The third peak in O1s spectra at 532.7 eV corresponds to the water molecules present on the surface.

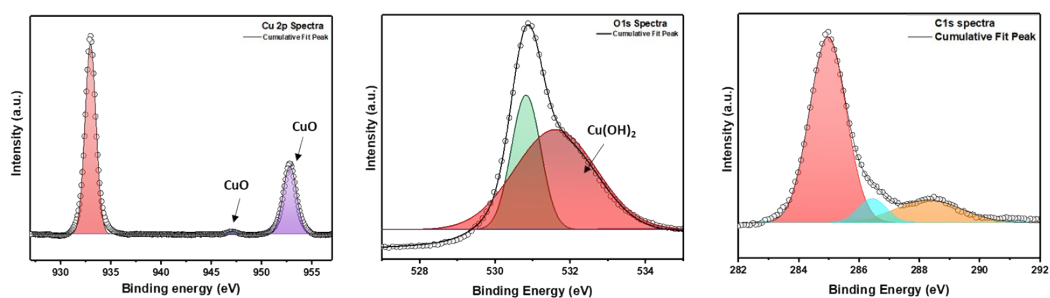


Figure S5: XPS spectra of bare Cu

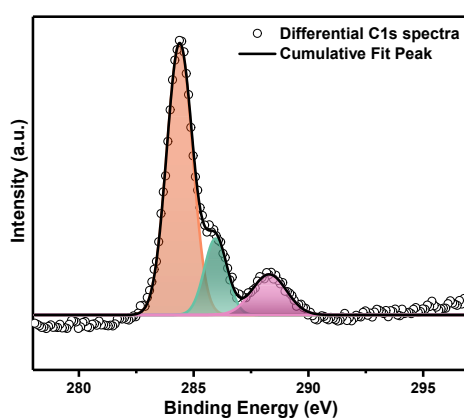


Figure S6: Differential C1s spectra by subtracting the C1s spectra of bare Cu from silanized Cu.

- Quantification of the XPS Spectrum of bare Cu, silanized Cu, and TNS-coated Cu

Table S1: Quantification of the XPS Spectrum of bare Cu

| S.no. | Peak | Peak position | Species | Area % |
|-------|------------------|---------------|----------------------|--------|
| 1 | C _{1s} | 285 | C-C | 76 |
| | | 286.4 | C-C/C-H | 7 |
| | | 288.3 | C-C=O | 17 |
| 2 | Cu _{2p} | 933 | Cu | 69 |
| | | 947.1 | CuO | 1 |
| | | 952.8 | CuO | 30 |
| 3 | O _{1s} | 530.9 | Cu (OH) ₂ | 68 |
| | | 532.1 | Cu (OH) ₂ | 13 |
| | | 532.7 | H ₂ O | 20 |

Table S2: Quantification of the XPS Spectrum of Silanized Cu

| S.no. | Peak | Peak position | Species | Area % |
|-------|------------------|---------------|------------------------|--------|
| 1 | N _{1s} | 399.9 | free NH ₂ | 91 |
| | | 398.4 | bonded NH ₂ | 9 |
| 2 | C _{1s} | 284.7 | C-C/C-H | 74 |
| | | 286.2 | C-O/C-N | 12 |
| | | 288.3 | C-C=O | 14 |
| 3 | Cu _{2p} | 932.9 | Cu | 34 |
| | | 933.9 | Cu-O | 28 |
| | | 941.4 | Cu-O | 3 |
| | | 942.6 | Cu-O | 0 |
| | | 944.1 | Cu-O | 3 |
| | | 952.7 | Cu-O | 15 |
| | | 953.8 | Cu-O | 15 |
| | | 962.6 | Cu-O | 2 |
| 4 | O _{1s} | 530.3 | Cu(OH) ₂ | 12 |
| | | 533.4 | C-O/C-N | 6 |
| | | 531.7 | Cu-O | 82 |
| 5 | Si _{2p} | 102.2 | Si)-Cu | 100 |

Table S3: Quantification of the XPS Spectrum of TNS-coated Cu

| S.no. | Peak | Peak position | Species | Area % |
|-------|------------------|---------------|---------|--------|
| 1 | C _{1s} | 284.9 | C-C/C-H | 73 |
| | | 286.3 | C-O/C-N | 17 |
| | | 288.6 | C-C=O | 10 |
| 2 | Cu _{2p} | 932.8 | Cu | 27 |
| | | 934.8 | Cu-O | 29 |
| | | 942.2 | Cu-O | 10 |
| | | 944.4 | Cu-O | 4 |
| | | 952.6 | Cu-O | 13 |
| | | 954.7 | Cu-O | 12 |
| | | 962.9 | Cu-O | 5 |
| 3 | O _{1s} | 530.2 | Ti-O | 34 |
| | | 531.6 | Ti-O | 66 |
| 4 | Ti _{2p} | 458.6 | Ti-O | 70 |
| | | 464.3 | Ti-O | 30 |
| 5 | B _{1s} | 192 | B-O | 95 |
| | | 193.1 | B-O | 5 |

5. Mechanism: Electrostatic immobilization of TNS on Cu substrate

The deposition of TNS on Cu as explained from XPS results can be summarized as follows. First, the Cu surface gets hydroxylated by acid treatment. When the APTES molecules are introduced on the Cu substrate, the ethoxy groups in APTES molecules are hydrolyzed to form silanol (Si-O-H) groups. These silanol groups self-assemble on the Cu surface by forming a lateral (Cu-O-Si) network. When the negatively charged nanosheets are introduced they electrostatically attach to the positively charged NH_2 groups present on the silanized Cu surface.

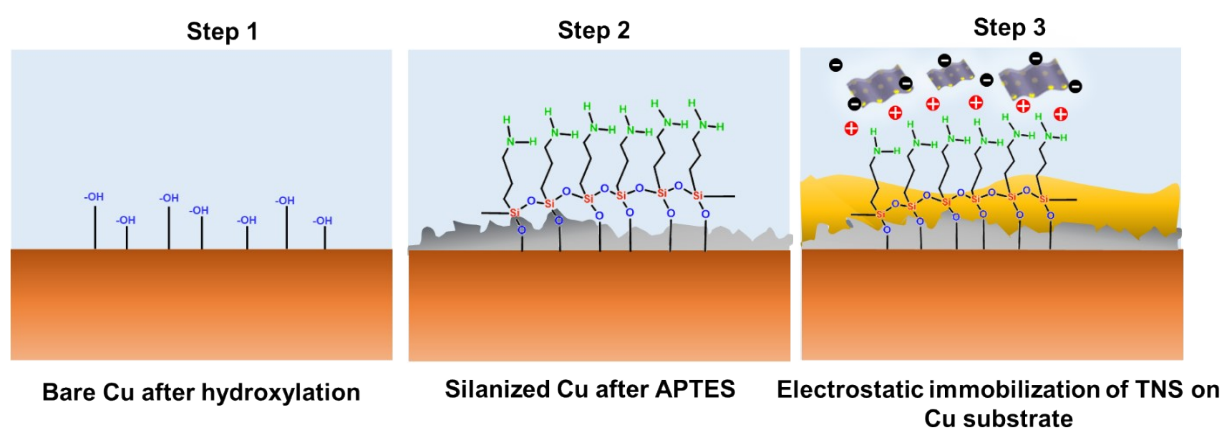


Figure S7: Step-by-step mechanism of electrostatic immobilization of TNS on Cu substrate

6. FE-SEM images of bare Cu and TNS-coated Cu.

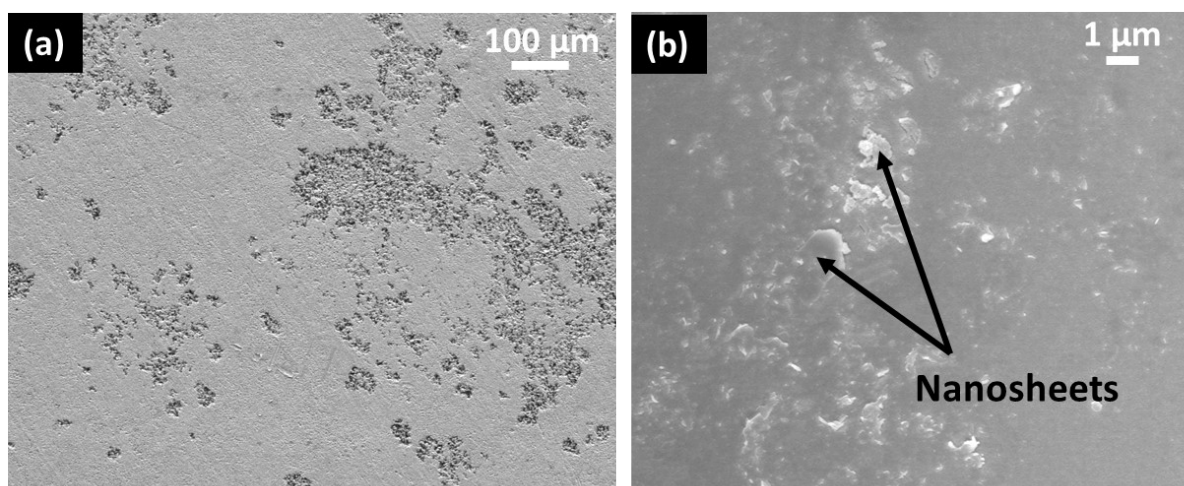


Figure S8: FE-SEM images of (a) bare Cu and (b) TNS-coated Cu

7. EDX analysis of TNS-coated Cu

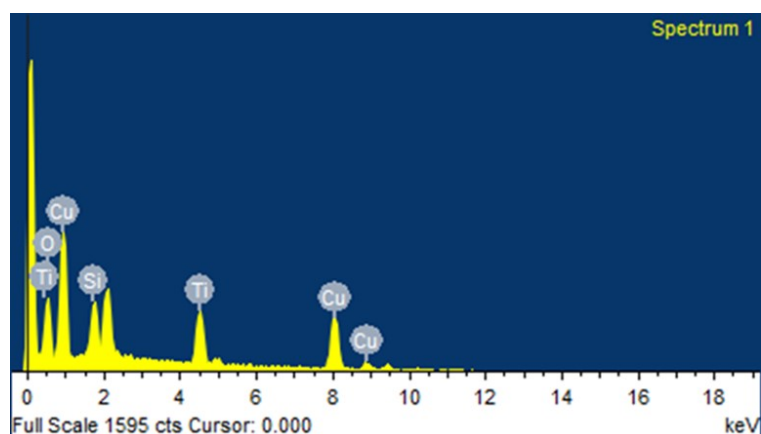


Figure S9: EDX analysis of TNS-coated Cu

Table S4: Elemental analysis of TNS-coated Cu

| Element | Weight% | Atomic% |
|---------|---------|---------|
| O K | 28.86 | 56.88 |
| Si K | 8.32 | 9.34 |
| Ti K | 16.08 | 10.59 |
| Cu L | 46.73 | 23.19 |

8. Determination of coating thickness AFM images and height profile.

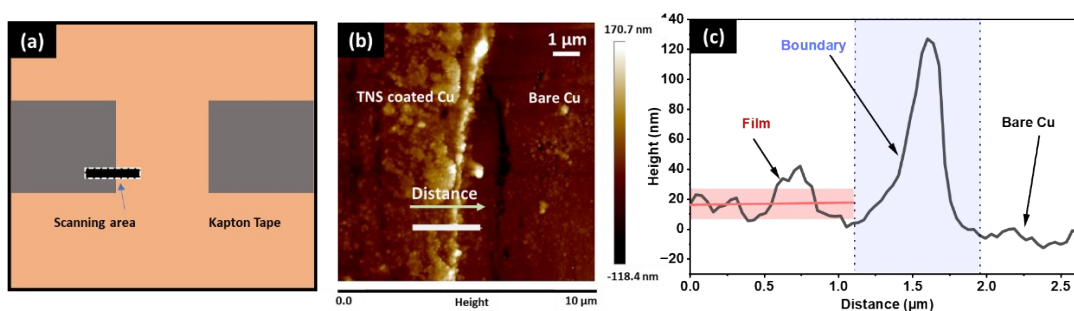


Figure S10: AFM scanning to determine the thickness of the TNS-coated Cu: Coating thickness measurement using AFM scan of the boundary and its corresponding height profile indicating the thickness of the film to be less than 100 nm.

9. Contact angle images

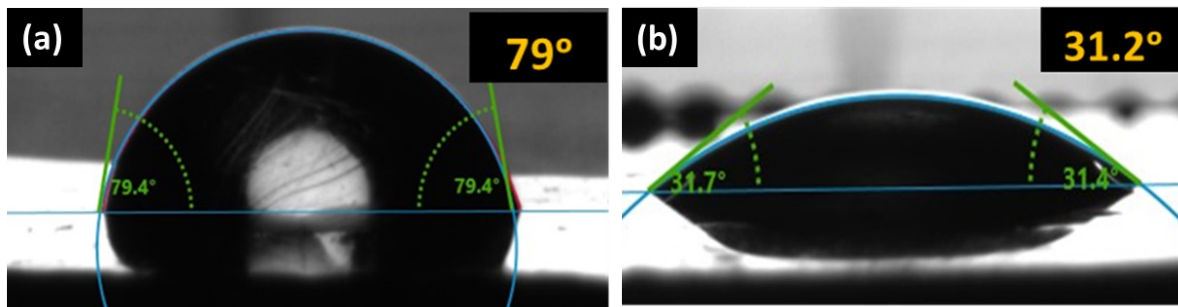


Figure S11: Contact angle measurements of (a) bare Cu and (b) TNS-coated Cu exhibit enhanced hydrophilicity after coating.

10. Calculation of surface energy

Table S5: Polar and Dispersive Surface Energy Components of the Test Liquids

| Test liquid | γ_l (mJ/m ²) | γ_l^p (mJ/m ²) | γ_l^d (mJ/m ²) |
|----------------------|---------------------------------|-----------------------------------|-----------------------------------|
| Water (W) | 72.8 | 51 | 21.8 |
| Diiodomethane (DIM) | 50.8 | 0 | 50.8 |
| Ethylene Glycol (EG) | 48 | 19 | 29 |
| Glycerol (G) | 64 | 30 | 34 |

Fowkes Model: Fowkes surface energy theory integrates the Young and Young–Dupree equations and separates the liquid and solid surface energy into its polar and nonpolar (dispersive) components.

$$\frac{\gamma_l(\cos\theta + 1)}{2} = (\gamma_l^d)^{1/2} (\gamma_s^d)^{1/2} + (\gamma_l^p)^{1/2} (\gamma_s^p)^{1/2} \dots\dots\dots(1)$$

$$\gamma_s = \gamma_s^d + \gamma_s^p \dots\dots\dots(2)$$

where,

- γ_l^d = surface energy of the liquid dispersive component
- γ_l^p = surface energy of liquid polar components
- γ_s^d = surface energy of the solid dispersive component
- γ_s^p = surface energy of solid polar components

Steps:

- In this method, surface energy is calculated using 2 test liquids - water and Diiodomethane (DIM).
- First, we calculated the γ_s^d value by putting the standard surface energy values of the liquid component of DIM from Table S3 in eq.1.
- Second, we calculated the γ_s^l value by putting the standard surface energy values of the liquid component of water and the calculated γ_s^d value in eq.1.
- Subsequently, we calculated the total surface energy (γ_s) by using eq.2, as this theory assumes that the γ_s is the sum of the polar and dispersive components of a solid surface.

Owens-Wendt (Extended Fowkes) Model: This model is the extension of the Fowkes model by incorporating Good's equation. ²

$$\gamma_{sl} = \gamma_s + \gamma_l - 2(\gamma_s^d \gamma_l^d)^{1/2} - 2(\gamma_s^p \gamma_l^p)^{1/2} \dots\dots\dots(3)$$

$$\frac{\gamma_l(\cos\theta + 1)}{2((\gamma_l^d)^{1/2})} = \frac{(\gamma_s^p)^{1/2}}{(\gamma_l^p)^{1/2}} + (\gamma_s^d)^{1/2} \dots\dots\dots(4)$$

γ_{sl} = surface energy at the solid–liquid interface.

Steps:

- The polar and dispersive components of the liquid surface energy is known.
- We plotted the left side of Eq. 4 against $\frac{(\gamma_l^p)^{1/2}}{(\gamma_l^d)^{1/2}}$, this yields a linear trend of data points.
- We performed the linear regression on this data and obtained the γ_s^p as the square of the slope and γ_s^d as the square of the y-intercept.

11. Calculation of contact angle hysteresis (CAH)

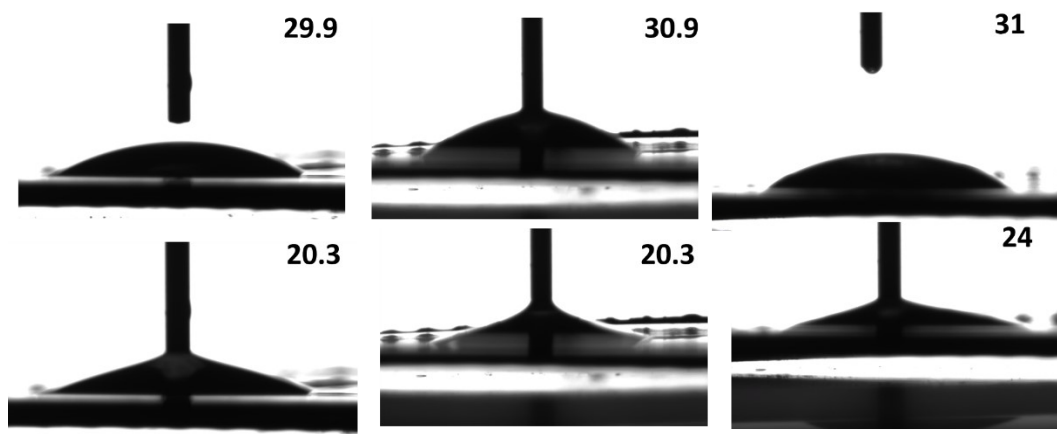


Figure S12: Contact angle images of TNS-coated Cu

Table S6: Calculation of contact angle hysteresis (CAH)

| Samples | CAH | Mean | Standard deviation |
|---------------|-------|-------|--------------------|
| Bare Cu | 72.37 | | |
| | 54.6 | 59.73 | 11 |
| | 52.23 | | |
| | 35.18 | | |
| Silanized Cu | 43.92 | 41.14 | 5.16 |
| | 44.32 | | |
| TNS-coated Cu | 9.61 | | |
| | 10.62 | 9.08 | 1.86 |
| | 7.02 | | |

12. Condensation experiment

In this study, our focus is primarily on establishing a new family of two-dimensional materials as coating surfaces for condensation. Therefore, we selected 75% RH as a representative to evaluate the condensation behavior of the TNS-coated Cu surface in comparison with bare Cu (Figure S13a). We assume that the qualitative trend reported for this RH value would remain

similar for other RH values as well. As evidence we performed condensation experiment at 80% RH value as well (Figure S13b). We found that at 10 °C, the bare Cu performs better than the TNS-coated Cu; however, at 20 °C, the TNS-coated Cu outperforms the bare Cu. This trend is similar to the results obtained at 75% RH. (The comparative graph is shown in Figure S13, in which we have shown the calculated heat flux value at 75% and 80% RH value).

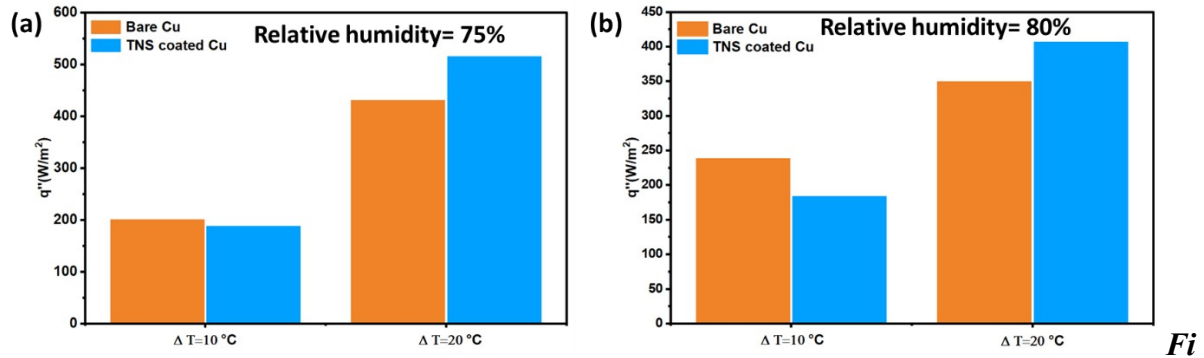


Figure S13: Condensation heat flux, q'' (solid bars) on bare Cu and TNS-coated Cu surfaces at relative humidity (RH) values (a) 75%, and (b) 80%.

Reference

- 1 A. L. James, M. Lenka, N. Pandey, A. Ojha, A. Kumar, R. Saraswat, P. Thareja, V. Krishnan and K. Jasuja, *Nanoscale*, 2020, **12**, 17121–17131.
- 2 A. Kozbial, Z. Li, C. Conaway, R. McGinley, S. Dhingra, V. Vahdat, F. Zhou, B. D’Urso, H. Liu and L. Li, *Langmuir*, 2014, **30**, 8598–8606.